Jurnal Polimesin
Department of Mechanical Engineering
State Polytechnic of Lhokseumawe
http://e-jurnal.pnl.ac.id/polimesin

e-ISSN : 2549-1999 No. : 2 Month : April
p-ISSN : 1693-5462 Volume : 21 Year : 2023

Article Processing Dates: Received on 2023-02-07, Reviewed on 2023-03-09, Revised on 2023-04-10, Accepted on 2023-04-11 and Available online on 2023-04-25

Development of CFD simulation model of earth air heat exchanger for space cooling of a 36 m^2 house in tropical climate Banda Aceh, Indonesia

Sarwo Edhy Sofyan[1*], Khairil[1], Zhafran Maulana[1], Akram Tamlicha[1], Jalaluddin[1], M. Syaukani[2]
[1]Department of Mechanical Engineering, Universitas Syiah Kuala, Banda Aceh, 23111, Indonesia
[2]Program Study of Mechanical Engineering, Department of Production and Industrial Technology, Institut Teknologi Sumatera, South Lampung, 3536, Indonesia
*Corresponding author: sarwo.edhy@usk.ac.id

Abstract

The global warming makes the ambient temperature hotter and greater efforts are made to reach a comfortable temperature. The continuous use of air conditioners that consume electricity is also unsustainable for the surrounding environment. Several studies on thermal comfort have been conducted by various researchers. Earth-air heat exchangers (EAHE) with air-working fluids can be used as a passive contribution to reduce building energy requirements for heating or cooling purposes. It should be noted that there is very little information in the literature on the development of a CFD (Computational Fluid Dynamic) simulation model of an EAHE for space cooling of a 36 m^2 house in a tropical climate, such as Banda Aceh, Indonesia. Therefore, this study aims to examine the performance of EAHE with several variations in design parameters, such as pipe length, pipe diameter, number of pipe bends, and the type of soil where the EAHE is installed, as well as the thermal regime of a 36 m^2 house either with or without the use of EAHE. The simulation in this study was conducted with CFD ANSYS Fluent software. The inlet air temperature of EAHE was set to be the same as the ambient air temperature, namely 31.4^{o}C. The simulation results reveal that for variations in pipe length, the highest drop in outlet air temperature was yielded by the 47 m pipe length, which is 26.8°C. In which an increase in pipe length causes a decrease in air outlet temperature. The variation in pipe diameter does not significantly affect the outlet air temperature. Where the average air temperature drop at the EAHE exit is 0.046^{o}C. The variation in number of turns shows that the drop in outlet air temperature is identical, namely 28.2°C, despite the fact that their pressure drop values are different. In addition, it was found that the performance of EAHE buried under different types of soil is distinct. The highest drop in outlet air temperature was generated when the EAHE was buried in silty soil, namely 26.1°C. A case study on a 36 m^2 house shows that the utilization an underground heat exchanger can reduce the house's indoor temperature by 2°C, with an average house temperature of 30.4°C compared to that with a natural ventilation.

Keywords:
Earth-air heat exchanger, Air conditioning, CFD, 36 m^2 house.

1 Introduction

The average surface temperature of the earth has increased by about 0.74°C in the last 100 years. Many experts estimate that the average temperature will increase from 1.4°C to 5.8°C by 2100. Meanwhile, the Intergovernmental Panel on Climate Change (IPCC) predicts that global temperatures are likely to increase by 1.1°C to 6.4°C in the next 90 years [1]

Airflow with an open loop in earth-air heat exchangers (EAHE) can be used as a passive contribution to reducing building energy demand for heating and cooling, by providing thermal pre-cooling from ventilation air as needed [2]. This is in line with Indonesian government policy, which is gradually expanding the energy-saving label program and Minimum Energy Performance Standards (MEPS) by phasing out energy-intensive household appliance technology. By implementing this energy policy, the government intends to be self-sufficient in meeting future energy demands and to ensure national energy security in the face of global change [3, 4].

Earth-air heat exchangers (EAHE) are made up of one or more pipes that are buried in the ground and are used to cool buildings. The phenomenon that occurs is quite simple and depends on the temperature difference between the soil and the ambient air. When ambient air is flowed into pipes buried underground, it experiences direct heat transfer with the surrounding soil [5, 6]. Experimental research was conducted in North Sumatra on earth-air heat exchangers (EAHE) as air conditioners with a closed loop system, with EAHE pipes buried at a depth of 2 m, with a pipe length of 26.5 m, a pipe diameter of 0.1016 m and a thickness of 0.003 m. The testing process was carried out starting at 10.00 a.m. until 06.00 p.m. with an inlet air flow rate of 2 m/s and 3 m/s, the results obtained were decreases in temperature in the test room ranging from 3-6 °C [7].

1.1 Mathematical Modelling

The total heat transfer from the air as it flows through a pipe buried in the ground is Eq. 1:

$$Q = \dot{m}_{air} C_{p,air} (T_{air,out} - T_{air,in}) \quad (1)$$

Due to convection between the pipe walls and the air, the heat transfer equation can also be written as Eq. 2:

$$Q = hA\Delta T_{lm} \quad (2)$$

Logarithmic mean temperature difference logaritmik (Eq. 3), $T_{ground} = T_{wall}$

$$T_{lm} = \frac{T_{in} - T_{out}}{ln\left[\frac{T_{in} - T_{wall}}{T_{out} - T_{wall}}\right]} \quad (3)$$

The mathematical model of subsurface soil temperature is based on the theory of heat conduction applied to semi-infite homogeneous solids. Soil temperature predictions show a sinusoidal pattern due to annual fluctuations [8]. To obtain the soil temperature at a certain depth, the following equation was used (Eq. 4):

$$T(z,t) = T_{meam} + Acos\left[\omega(t - t_0) - \frac{z}{d}\right] \times exp(-\frac{z}{d}) \quad (4)$$

The fundamental equations for fluid flow and heat transfer are generally governed by three conservation laws, namely the equations of continuity, conservation of momentum, and conservation of energy [9]:

Continuity equation:

$$\frac{\partial u}{\partial x} + \frac{\partial v}{\partial y} + \frac{\partial w}{\partial z} = 0 \quad (5)$$

.

X-momentum equation:

$$\left[u\frac{\partial u}{\partial x}+v\frac{\partial u}{\partial y}+w\frac{\partial u}{\partial z}\right]=-\frac{1}{\rho}\frac{\partial P}{\partial x}+\vartheta\left[\frac{\partial^2 u}{\partial x^2}+\frac{\partial^2 u}{\partial y^2}+\frac{\partial^2 u}{\partial z^2}\right] \quad (6)$$

Y-momentum equation:

$$\left[u\frac{\partial v}{\partial x}+v\frac{\partial v}{\partial y}+w\frac{\partial v}{\partial z}\right]=-\frac{1}{\rho}\frac{\partial P}{\partial y}+\vartheta\left[\frac{\partial^2 v}{\partial x^2}+\frac{\partial^2 v}{\partial y^2}+\frac{\partial^2 v}{\partial z^2}\right] \quad (7)$$

Z-*momentum equation:*

$$\left[u\frac{\partial w}{\partial x}+v\frac{\partial w}{\partial y}+w\frac{\partial w}{\partial z}\right]=-\frac{1}{\rho}\frac{\partial P}{\partial z}+\vartheta\left[\frac{\partial^2 w}{\partial x^2}+\frac{\partial^2 w}{\partial y^2}+\frac{\partial^2 w}{\partial z^2}\right] \quad (8)$$

Energy conservation equation:

$$\left[u\frac{\partial T}{\partial x}+v\frac{\partial T}{\partial y}+w\frac{\partial T}{\partial z}\right]=\alpha\left[\frac{\partial^2 T}{\partial x^2}+\frac{\partial^2 T}{\partial y^2}+\frac{\partial^2 T}{\partial z^2}\right] \quad (9)$$

In the Eq. 5-9. u, v, and w are the velocity components in the x, y, and z directions, P and T are the pressure and temperature of the flowing air, ϑ is the kinematic viscosity, and α is the thermal diffusivity of the soil.

Conjugate Heat Transfer (CHT) allows the simulation of heat transfer between solid and fluid domains by exchanging heat energy at the interface between the two. Applications of this type exist, such as in heat exchanger simulation, electronic equipment cooling, and general purpose cooling and heating systems [10, 11]. In Conjugate Heat Transfer (CHT) the model used is:

- Energy equation (on)
- Viscous (Realizable K-epsilon)

The energy equation used is Eq. 10:

$$\frac{\partial}{\partial t}(\rho E)+\nabla\cdot\left(\vec{\vartheta}(\rho E+p)\right)=\nabla\cdot\left(k_{eff}\nabla T-\sum_j h_j\vec{J}_j+\left(\bar{\bar{\tau}}_{eff}\cdot\vec{\vartheta}\right)\right)+S_h \quad (10)$$

Where k_{eff} is the effective conductivity (k + kt, with kt is the turbulent thermal conductivity, determined according to the turbulence model used), and $\vec{J}_j$ is the species diffusion flux j. The first three terms on the right-hand side of the equation represent energy transfer due to conduction, diffusion of species, and viscous dissipation, respectively. S_h including heat of chemical reaction, and other specified volumetric heat sources [12]. The energy E per unit mass is defined as Eq. 11:

$$E=h-\frac{p}{\rho}+\frac{V^2}{2} \quad (11)$$

Turbulence models *K-epsilon* (*k-ε*) is the most commonly used model in Computational Fluid Dynamics (CFD) to simulate average flow characteristics for turbulent flow conditions. This is a two-equation model that provides an overview of turbulence through the two equations between turbulent kinetic energy *k* and dissipation *ε*. On Realizable models K-epsilon updated turbulent viscosity equation and new transport equation for dissipation rate, *ε* has been derived from the exact equation for the mean-squared vorticity fluctuation transport [12].

Turbulence kinetic energy (k) (Eq. 12):

$$\frac{\partial}{\partial t}(\rho k)+\frac{\partial}{\partial x_j}(\rho k u_j)=\frac{\partial}{\partial x_j}\left[\left(\mu+\frac{\mu_t}{\sigma_k}\right)\frac{\partial k}{\partial x_j}\right]+G_k+G_b-\rho\epsilon-Y_M+S_k \quad (12)$$

Dissipation rate (ε) (Eq.13)

$$\frac{\partial}{\partial t}(\rho\varepsilon)+\frac{\partial}{\partial x_j}(\rho\varepsilon u_j)=\frac{\partial}{\partial x_j}\left[\left(\mu+\frac{\mu_t}{\sigma_\varepsilon}\right)\frac{\partial\varepsilon}{\partial x_j}\right]+\rho C_1 S_\varepsilon-\rho C_2\frac{\varepsilon^2}{k+\sqrt{\nu\varepsilon}}+C_{1\varepsilon}\frac{\varepsilon}{k}C_{3\varepsilon}G_b+S_\varepsilon \quad (13)$$

Where,

$$C_1=max\left[0.43,\frac{\eta}{\eta+5}\right],\ \eta=S\frac{k}{\varepsilon},\ S=\sqrt{2S_{ij}S_{ij}} \quad (14)$$

This equation, G_k represents the derivative of the turbulence kinetic energy due to the average velocity gradient, G_b is the kinetic energy derivative of turbulence due to buoyancy, Y_M represents the contribution of the fluctuating dilation in compressible turbulence to the overall dissipation rate, C_2 and $C_{1\varepsilon}$ constan, σ_k and σ_ε each is a turbulent Prandtl number for k and ε. S_k and S_ε is a user-defined source term [12].

Room Temperature Simulation simulated heat transfer in airflow in a ventilated room. The model used in this simulation is:

- Energy equation (on)
- Viscous (SST k – omega)
- Solar load (Solar ray tracing)
- Bondary wall condition (Convective Heat transfer)

The energy equation used is the same as in equation (10). The turbulence model (SST k-omega) according to Paepe and Janssens [11, 13] models fluid flow in a ventilated room which has the closest results to the experimental data, so the turbulence model (SST k-omega) is very suitable for use in Room Temperature simulations.

The k-omega (k−ω) turbulence model is one of the most commonly used models to capture the effects of turbulent flow conditions. This is a two-equation model. That means in addition to the conservation equation, it solves two transport equations (PDE), which explain effects such as turbulent energy convection and diffusion. The two variables entered are the turbulent kinetic energy (k) which determines the energy in turbulence and the specific turbulence dissipation rate (ω) which determines the rate of dissipation per unit of turbulent kinetic energy, also referred to as the turbulence scale [12].

In the k-omega SST turbulence model, SST stands for shear stress transport. The SST formulation switches to the behavior of k−ϵ in free flow, which avoids the k−ω problem which is sensitive to the turbulent nature of incoming free flow. With the refinement of the equation as follows:

- The modified k–omega and k-epsilon standard models are both multiplied by the blend function and the two models are summed. The blending functions are designed to be one in the near-wall region, which activates the k–omega standard model and zero away from the surface which activates the k–modified epsilon.
- The SST model incorporates the damped cross-diffusion derivative term in the ω equation.
- The definition of turbulent viscosity is modified to account for the transport of turbulent shear stresses.
- The modeling constants are different.

The k–omega SST model has a shape similar to the standard k–omega model as shown in the following equation:

Turbulence kinetic energy (k) (Eq. 15)

$$\frac{\partial}{\partial t}(\rho k)+\frac{\partial}{\partial x_i}(\rho k u_i)=\frac{\partial}{\partial x_j}\left(\Gamma_k\frac{\partial k}{\partial x_j}\right)+\tilde{G}_k-Y_K+S_k \quad (15)$$

Specific turbulent dissipation rate (ω) (Eq. 16)

$$\frac{\partial}{\partial t}(\rho\omega)+\frac{\partial}{\partial x_i}(\rho\omega u_i)=\frac{\partial}{\partial x_j}\left(\Gamma_\omega\frac{\partial\omega}{\partial x_j}\right)+G_\omega-Y_\omega+D_\omega+S_\omega \quad (16)$$

In this equation, $\tilde{G}_k$ represents the generation of turbulence kinetic energy due to the average velocity gradient. G_ω represents the derivative of ω, Γ_k dan Γ_ω represents the effective diffusivity k and ω, respectively, which are calculated as described below. Y_K and Y_ω represent the dissipation of k and ω due to turbulence. D_ω represents the cross-diffusion term. S_k dan S_ω are user-defined source terms [12]. The effective diffusivity for the k–omega SST model is (Eq. 17-18):

$$\Gamma_k = \mu + \frac{\mu_t}{\sigma_k} \quad (17)$$

$$\Gamma_\omega = \mu + \frac{\mu_t}{\sigma_\omega} \quad (18)$$

Solar ray tracing can be used to predict the source of direct illumination energy resulting from incoming solar radiation. It takes the modeled beam using the sun's position vector and illumination parameters, applies it to any or all of your specified wall or inlet/outlet boundary zones, performs a surface shading analysis to determine well-defined shadows on all boundary surfaces and interior walls, and calculate the heat flux on the boundary surface resulting from incident radiation [12]. The equation for normal direct exposure using the Reasonable Weather Conditions Method is taken from ASHRAE (Eq. 19):

$$Edn = \frac{A}{e^{\frac{B}{sin(\beta)}}} \quad (19)$$

Where A and B are the apparent solar irradiance at air mass m = 0 and the atmospheric extension coefficient, respectively. These values are based on the Earth's surface on a sunny day. β is the sun's height (in degrees) above the horizontal.

The calculation of diffuse loads in the solar model is based on the approach suggested in ASHRAE 2001 (Chapter 20, Fenestrations). The equation for diffuse solar irradiation on a vertical surface is given by Eq. 20:

$$Ed = CY\ Edn \quad (20)$$

Where C is a constant whose values are given in Table 7 of Chapter 30 ASHRAE 2001, Y is the ratio of sky diffuse radiation on a vertical surface to that on a horizontal surface (calculated as a function of the angle of incidence), and Edn is the direct normal irradiance at the Earth's surface on a clear day [10].

The equation for diffuse solar irradiation for surfaces other than vertical surfaces is given Eq.21:

$$Edn = CEdn\frac{(1+cos\epsilon)}{2} \quad (21)$$

The equation for the solar irradiation reflected off the ground at the surface is given by Eq. 22:

$$\mathrm{Er} = \mathrm{Edn}(\mathrm{C} + \sin\beta)\rho_g\frac{(1-\cos\epsilon)}{2} \quad (22)$$

The total diffuse irradiation at a given surface will be the sum of Ed and Er when the input for diffuse solar irradiance is taken from the solar calculator. Otherwise, if the constant option is selected in the radiation dialog box, the total diffuse irradiation will be the same as specified in the dialog box.

1.2 Bondary wall condition (Convective Heat transfer)

Determining the boundary condition of the convection heat transfer coefficient at the wall, ANSYS FLUENT uses the input of the external heat transfer coefficient and the external heat sink temperature to calculate the heat flux to the wall (Eq. 23).

$$q = h_f(T_w - T_f) + q_{rad} = h_{ext}(T_{ext} - T_w) \quad (23)$$

Furthermore, it is noted that there is very little information available in the literature on earth-air heat exchangers (EAHE) for house coolers using CFD simulation [6]. Therefore, the purpose of this study was to study the earth-air heat on the influence of pipe length, pipe diameter, number of pipe bends, and the effect of the type of soil used in the earth-air heat exchanger and as well as to examine the application of house type-36.

2 Research method

In this study there are 2 simulations that will be carried out, the first is a simulation of an earth-air heat exchanger. After getting the results from the earth-air heat exchanger simulation, a type-36 house thermal regime simulation was carried out taking into account the cooling load from the house itself and then using air supply or without supply from the earth-air heat exchanger.

2.1 Geometry dimensions

2.1.1 Earth-air heat exchanger

The geometrical dimensions of the reference on the earth-air heat exchanger are as follows:

Table 1. The reference parameters of EAHE

Parameter	Value
Pipe length (m)	23
Pipe diameter (mm)	125
Spacing between pipes (m)	1

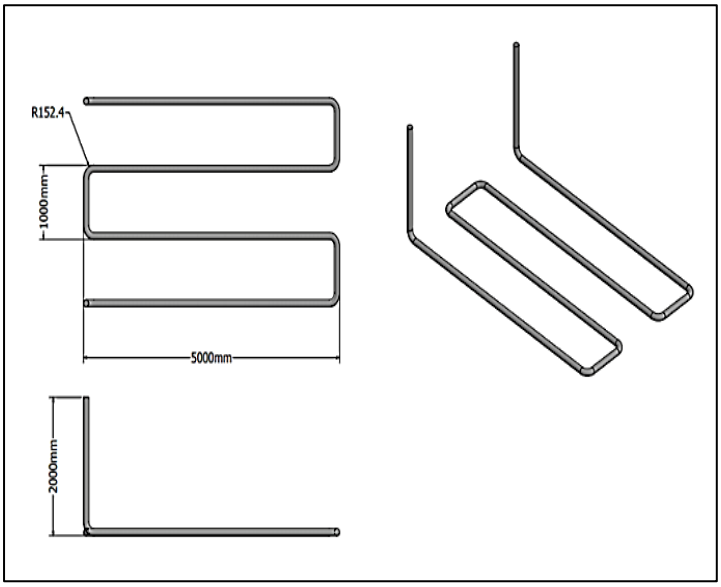

Fig. 1. Geometry dimensions of the earth-air heat exchanger.

2.1.2 Size type-36 house

The geometric dimensions of the type-36 house are as follows:

- Area of the house: 36 m^2 (6 m x 6 m)
- Wall thickness : 0,15 m
- Wall height : 3,2 m

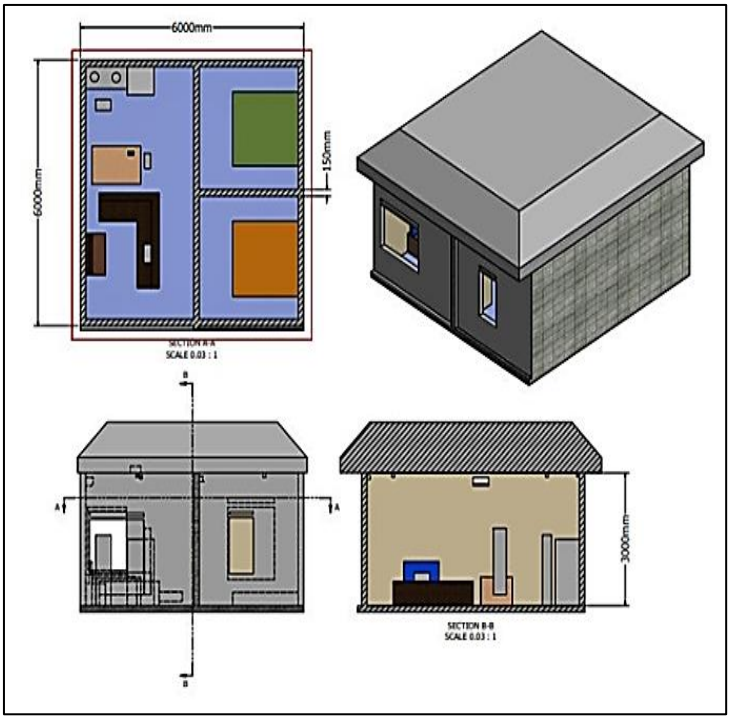

Fig. 2. Geometry dimensions of the house

2.2 Material

The materials used in this simulation are as follows:

a) Earth-air heat exchanger

Table 2. Material properties in EAHEs

Material	Density (kg/m^3)	Specific Heat (J/Kg.K)	Thermal conductivity (W/m.K)
Soil (Silt)	2000	1480	1
PVC	1400	1005	0.19

b) House type-36

Table 3. Material properties of the house

Material	Density (kg/m^3)	Specific Heat (J/Kg. K)	Thermal conductivity (W/m.K)	Absorptivity	Transmissivity
Wall	1800	900	0,8	0,3	-
Glass window	2600	840	0,96	0,5	0,8

2.3 Boundary conditions

The boundary conditions included in this simulation are as follows:

a) Earth-air heat exchanger
- Air mass flow rate = 0,04 kg/s
- Intake air temperature = 31,4 °C
- Soil temperature at z : 2 m = 25 °C

b) House type-36
- Solar radiation (coordinate location of Banda Aceh city)
  Longitude = 95,323753
  Latitude = 5,548290
- Month = June (10.00am–5.00pm) local time
- Internal cooling load
  - Lamp = 42 °C
  - TV = 40 °C
  - Human = 36,5 °C
- Air supply
  - 0,04 kg/s with an air temperature of 26.1 °C (supply of earth-air heat exchanger)
  - Natural ventilation with an air temperature of 31.4 °C (without heat exchanger supply)

3 Result and Dicussion

3.1 Effect of EAHE length on the outlet air temperature

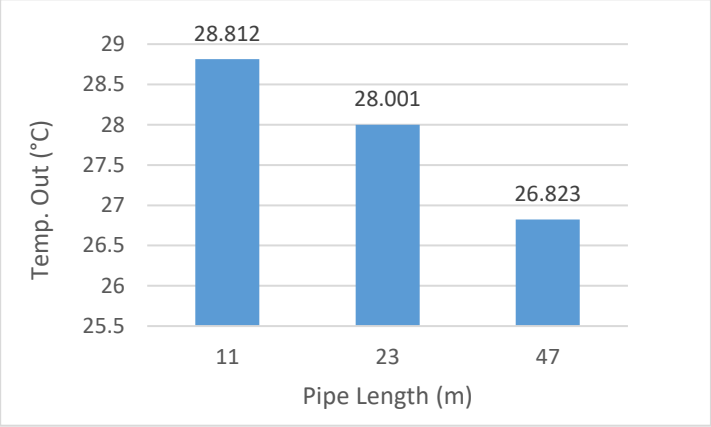

Fig. 3. The effect of the length of EAHE on the outlet air temperature

Fig 3 shows the relationship between the length of the EAHE and the outlet air temperature. It can be seen that the decrease in outlet air temperature is directly proportional to the length of the EAHE. The EAHE with 47 m long generates the lowest temperature drop namely of 26.823 °C, compared to those 11 m and 23 m length which yields 28,001 °C and 28.812 °C, respectively. This result summarises the outlet air temperature drop namely 2.6 °C, 3.4 °C, and 4.6 °C for 11 m, 23 m, and 47 m of EAHE length, respectively.

The effect of pipe length on EAHEs is that the longer the pipe, the longer the air passes through the heat transfer area so that the convection heat transfer that occurs is greater, this is in accordance with the convection heat transfer equation as shown in Eq. 2 that is $Q = hA\Delta T_{lm}$. Where the influencing variable is the cross-sectional area (A).

Table 4. Effect of earth-air Heat Exchanger Pipe Length

Pipe Diameter	Tout (°C)	ΔP	Va (m/s)
11 meter	28,812	29	3,08
23 meter	28,001	48,64	3,08
47 meter	26,823	91,557	3,08

From the Table 4, shows that the influence of the length of the earth-air heat exchanger pipe also affects the resulting pressure drop (ΔP), the longer the heat exchanger pipe, the greater the resulting pressure drop, the greater the need for a blower with greater power. The simulated air temperature contour for the influence of the pipe

length earth-air heat exchanger on the decreased air shown in Fig 4 below.

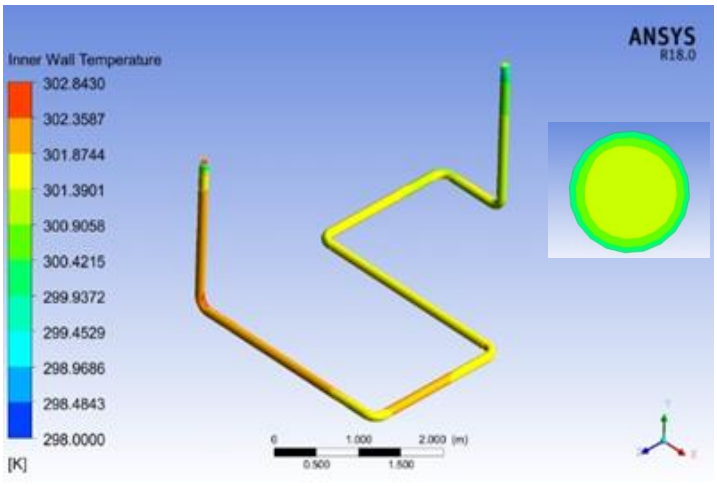

(a)

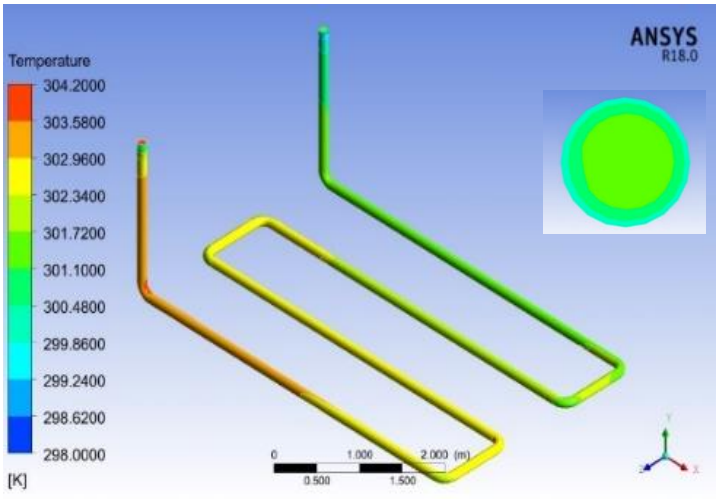

(b)

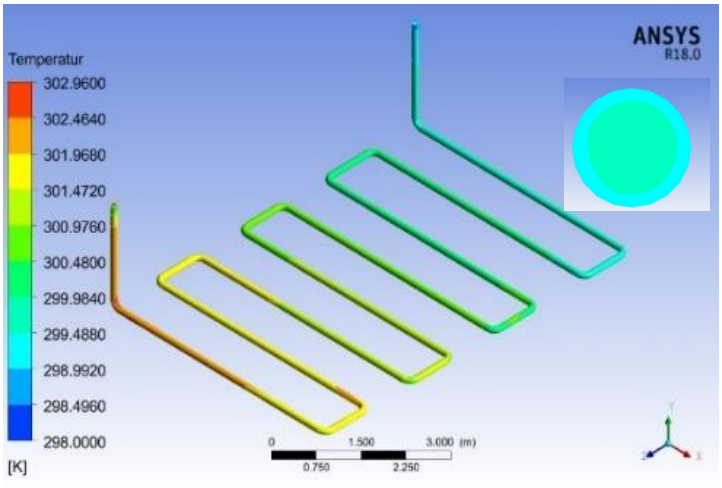

(c)

Fig. 4. Air temperature contour of the heat exchanger pipe (a) 11 meters pipe length, (b) 23 meters pipe length, and (c) 47 meters pipe length.

3.2 Effect of EAHE diameter on the outlet air temperature

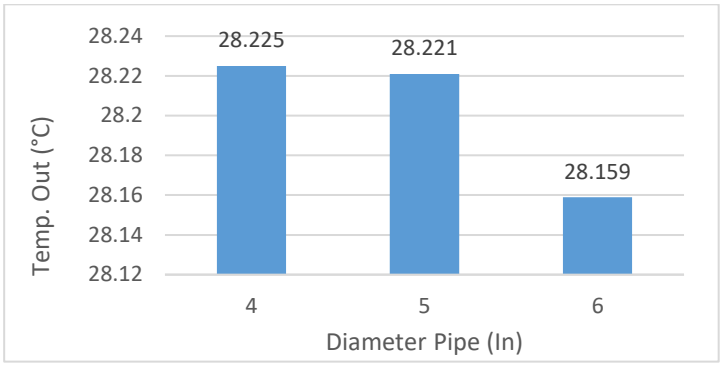

Fig 5. The effect of EAHE diameter on the outlet air temperature

Fig 5. shows the relationship between the pipe diameter of EAHE against air temperature at the outlet. The results show that the decrease in temperature is directly proportional to the increase in the diameter of the heat exchanger, although it does not decrease significantly.

Table 5. Effect of earth-air heat exchanger pipe diameter

Pipe Diameter	Tout (°C)	*ΔP*	Va (m/s)
4 inci	28,225	78	3,957
5 inci	28,221	45,34	3,06
6 inci	28,159	17,17	1,86

Table 5, shows the air velocity in the pipe (Va) is influenced by the pipe diameter. It was found that there is a decrease in air velocity of 53% for a 6-in pipe diameter and 23% for a 5-in pipe diameter compared to that is yielded by a 4-in diameter. This phenomenon affects convection heat transfer of EAHE. Actually, the larger the EAHE diameter, the thicker the air area that is not in direct contact with the heat transfer area. This trend renders the difference in temperature drop to be negligible, with an average temperature drop of 0.046 °C.

3.3 Effect of the number of EAHE turns on the outlet air temperature

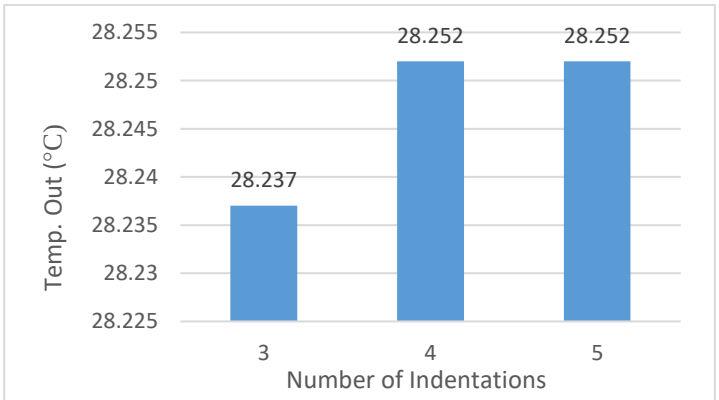

Fig. 6. The effect of number of EAHE turns on the outlet air temperature

Fig 6 shows the relationship between the number of bends in the EAHE and the outlet air temperature. The results demonstrate that

the decrease in air temperature is insignificant for the addition of the number of turns of EAHE.

Table 6. Effect of the number of turns of EAHE

Number of Indentations	Tout (°C)	*ΔP*	*Va (m/s)*
3	28,237	80	3,96
4	28,252	83,54	3,96
5	28,252	87,26	3,96

Table 6 presents the EAHE's simulation results for three different number of turns. It was found that the number of indentations does not significantly affect the outlet air temperature of EAHE except the pressure drop. More number of turns lead to greater pressure drop. The deviation in pressure drop for every addition of 1 indentation was about ± 3.5 Pa. This will affect the blower power required to circulate air into the EAHE. The results suggest that proper design of EAHE is vital for energy efficiency.

3.4 Effect of soil type on EAHE's outlet air temperature

The performance of the EAHE installed in different types of soil was examined. Table 7 shows the thermal properties for different types of soil.

Table 7. Thermal properties of typical soil

Material	Density (kg/m^3)	Specific Heat (J/Kg.K)	Thermal conductivity (W/m.K)
Silt	2000	1480	1
Clay	1300	1004	1.3
Sand	1615	1140	1.125

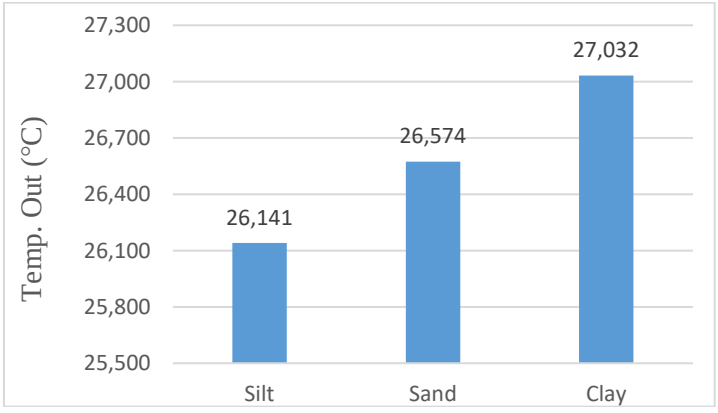

Fig 7. The effect of soil type on EAHE outlet air temperature

Fig 7 shows the relationship between the type of soil where the EAHE is installed and the outlet air temperature. The results show that the outlet air temperatures are 26.141°C for silt, 26.574°C for sand, and 27.032°C for clay. The thermal diffusivity for each type of soil affects the heat transfer capacity of EAHE. Using Eq. thermal diffusivity ie: $\propto = \frac{k}{\rho c_p}$, the results of the thermal diffusivity of each soil type were silt (α) = 3.37x10^{-7} m^2/s, sand (α) = 6.11x10^{-7} m^2/s, and clay α = 9.96x10^{-7} m^2/s respectively. It can conclude that the smaller the thermal diffusivity of the material used, the better the temperature drop will be.

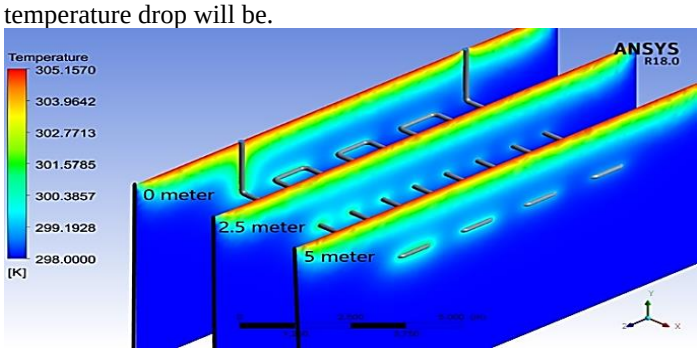

Fig 8. Soil temperature contour on the vertical section.

Fig 8 shows the vertical sections of EAHE domain for three different distance namely, at 0 m, 2.5 m, and 5 m to present the thermal regime around the EAHE.

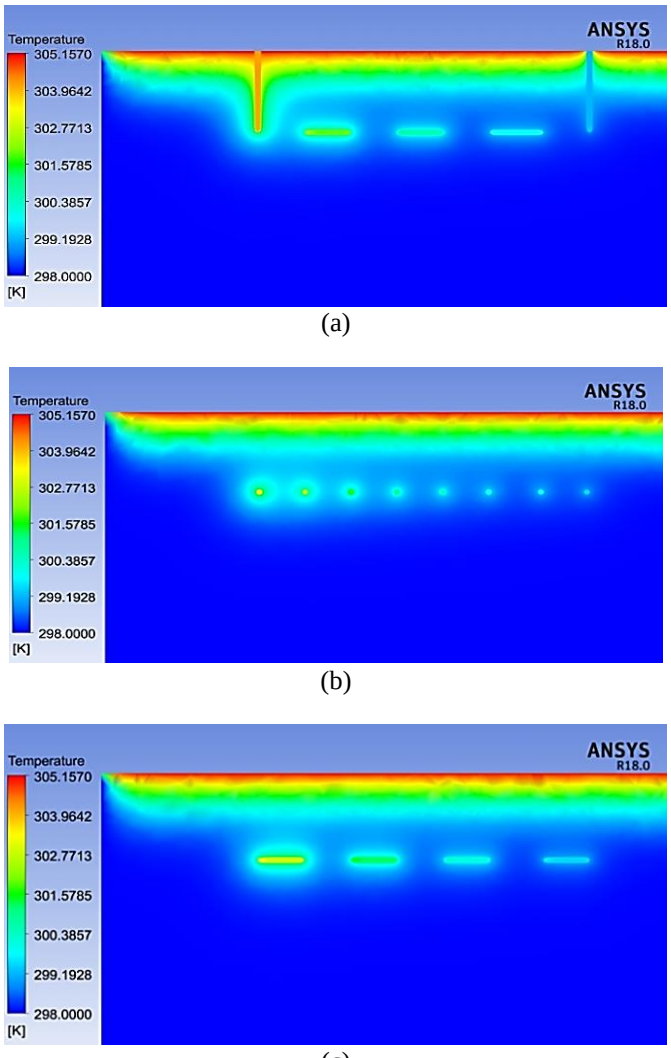

(a)

(b)

(c)

Fig 9. Soil temperature contour on the vertical section of inlet and outlet (a) 0 m section, (b) 2.5 m section, and (c) 5 m section.

Fig 9 presents each vertical section of EAHE domain at a distance 0 m, 2.5 m, and 5 m, respectively. The contour of soil temperature distribution is easier to observe at a point of 2.5 m. As it can be observed from the Fig that as the length of EAHE increases, the air temperature has decreased due to heat dissipation to the adjacent soil.

Solar radiation emitted to the ground surface generates heat which is then absorbed into the ground to a depth of ± 1 meter. Thus, it can conclude that the heat caused by solar radiation only propagates to a depth of ± 1 meter, and does not affect the soil at a

depth of 2 m where the soil at a depth of 2 m is used as an EAHE heat sink.

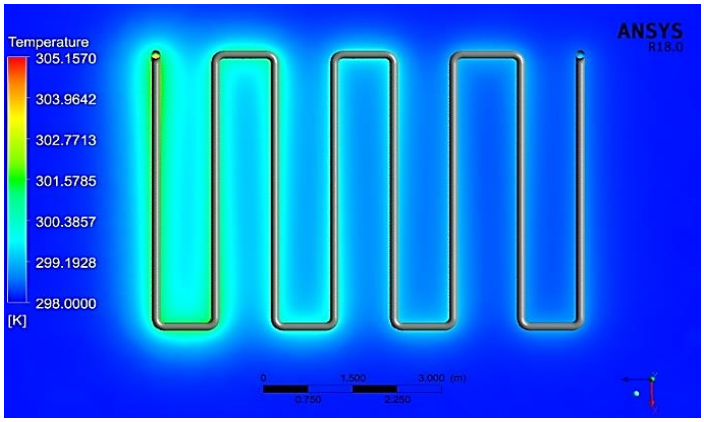

Fig 10. Horizontal section temperature contour at a depth of 2 meters

Fig 10 shows the thermal regime of EAHE at the top view section. It can be seen that the significant region with heat flow due to EAHE's heat dissipation is only for the area only ± 12 m along EAHE. The average soil temperature around the EAHE is ± 26.65 °C. The increase in soil temperature is only ± 1.65 °C from the initial temperature of 25 °C.

3.5 Case study of EAHE for cooling of a 36 m^2 house

The simulation of the thermal regime of the type-36 house has the following initial fixed parameters:

Mass flow rate : 0,04 kg/s
Air temperature : 27.2 °C (using the results of an earth-air heat exchanger with a pipe length of 47 meters and diameter 5 inches)
Solar radiation : Banda Aceh area with the front of the house facing south and the right side of the house facing east
Method : Transient (10.00am – 05.00pm)

3.5.1 Air requirement

According to the results of previous studies, the need for clean air for everyone living in the room is as much as 27 m^3/person/hour to 50 m^3/person/hour [14]. From the air requirement above, we average the air quality requirement at 38.5 m^3/person/hour = 0.01069 m^3/person/second. The number of people in the simulation was 3 people. So that, the air requirement was obtained at 0.01069 m^3/s x 3 = 0.03207 m^3/s, from the simulation the air mass flow rate ($\dot{m}$) which 0.04 kg/s, then 0.03207 m^3/s of air was converted to a mass flow rate about 0.0392 kg/s of air with Eq (2.8). Then, the air input to the house fulfilled by 0.0392 kg/s < 0.04 kg/s.

3.5.2 Inlet Air

The inlet used a square measuring 0.3 m x 0.15 m with an air mass flow rate of 0.04 kg/s resulting in an airflow rate of ± 0.4 m/s. The inlet in this simulation is only the supply air from the EAHE, while the ventilation, and the infiltration of the house are considered closed. According to ASHRAE 2001 [15, 16], for an airflow rate of 0.5 m/s or less and the incoming air temperature is not too cold. In this study, a bottom inlet for air supply is used as shown in Fig 11.

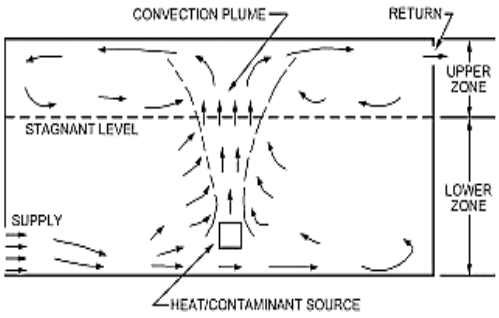

Fig 11. Intake air schematic [15].

3.5.3 Airflow

Fig 12 shows a comparison of the airflow into the house for a house with an EAHE supply and that with natural ventilation (without an EAHE supply).

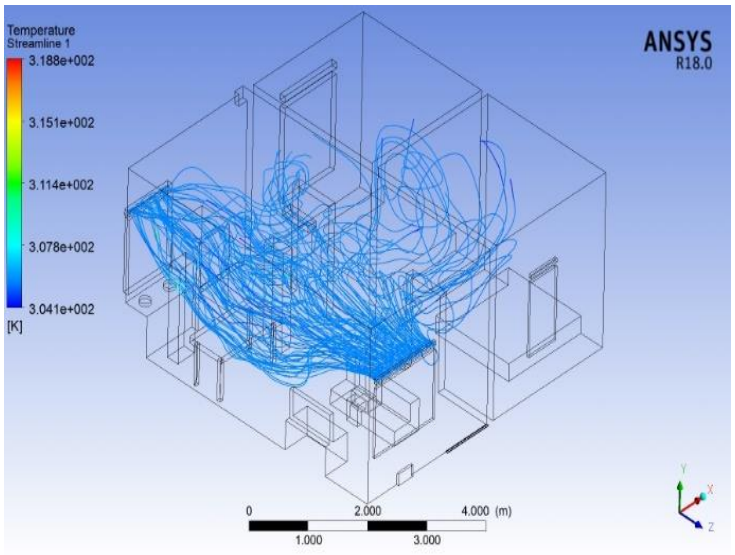

(a)

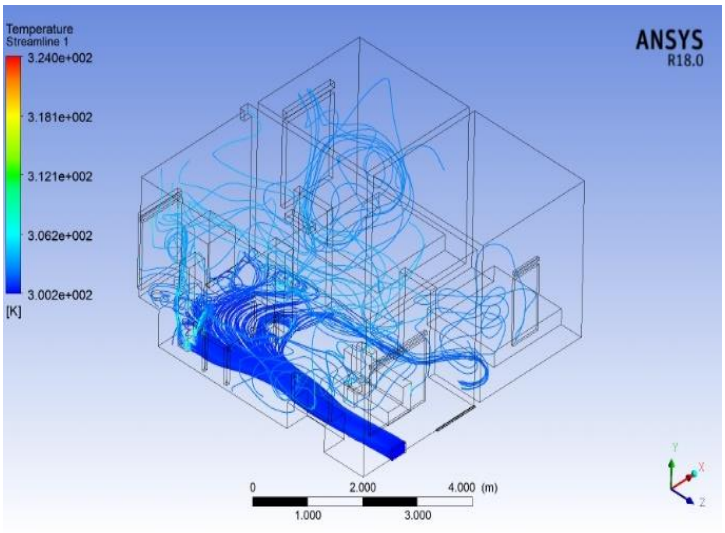

(b)

Fig 12. Airflow in a house (a) a house with natural ventilation (without EAHE supply), and (b) a house with EAHE supply.

Fig 12 illustrates a comparison of airflow inside the house with EAHE and natural ventilation. As we can see from Fig 12. (a) that the incoming air flow from the ventilation only passes through the top region instead of bootom of the house. Meanwhile when utilizing EAHE, the airflow entering through the inlet at the bottom region of the house, then the airflow rotates upwards to fill the house.

3.5.4 Indoor air temperature

As shown in Fig 13, it can be seen that the indoor air temperature for the case of natural ventilation (without supply air from EAHE) from 11.00 am – 05.00 pm that the highest temperature was obtained at 33.6°C on 04.00 pm at a height of 3 m and the lowest temperature was obtained 32.2°C at 12.00 am at a height of 0.5 m. From the Fig, it can be seen that the temperature inside the house was almost stable which was about 32 - 32.5 °C from 11.00 am - 02.00 pm, the increased temperature began at 03.00 pm - 05.00 pm which is 32.5 - 33.5 °C.

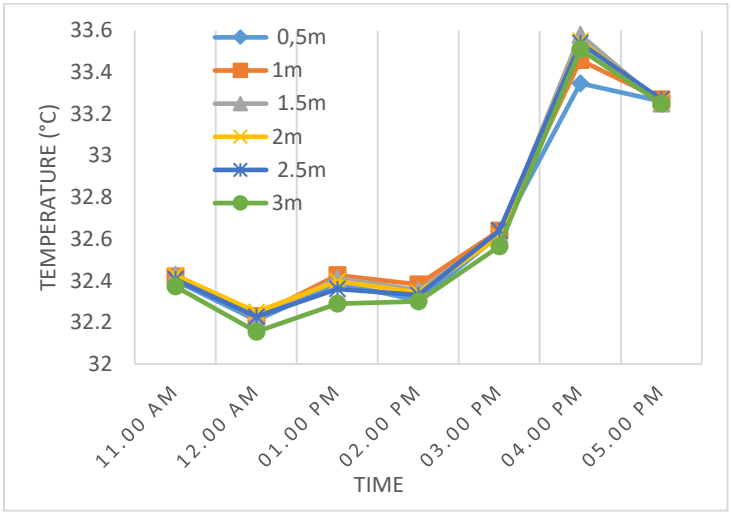

Fig 13. The average air temperature in a house with natural ventilation (without EAHE supply)

Fig 14 shown the indoor air temperature when the house equipped with EAHE during 11.00am - 05.00 pm. It is observed that the highest temperature was obtained at 31.65 °C on 05.00 pm at an elevation of 3 m. The lowest temperature obtained was 29.15°C on 02.00 pm at an altitude of 0.5 m. From the Fig it shows that the lowest temperature occurs at 0.5 - 1 m heigh. This tendency is to location of the air supply from the EAHE lies on the bottom wall that affects the thermal regime of the house.

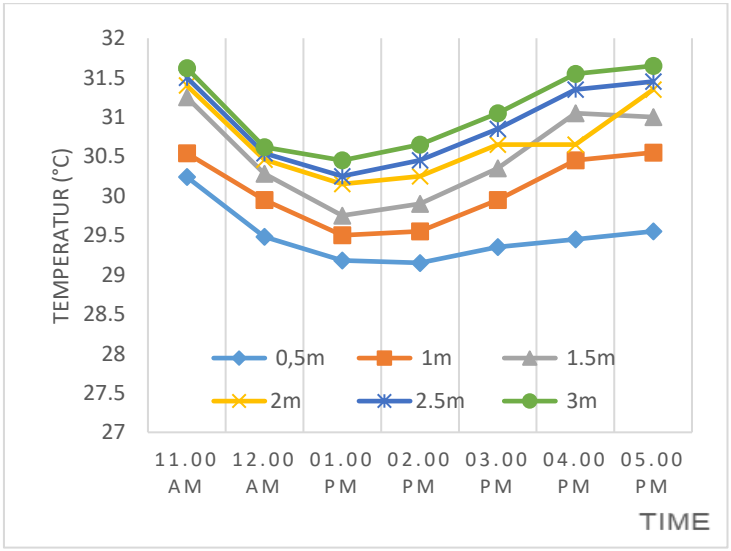

Fig 14. The average air temperature in a house supplied by an EAHE

4 Conclusion

There are several conclusions that can be drawn from this research. The effect of technical parameters shows that the outlet air temperature decreased directly proportional to the increase in pipe length. This is due to the larger surface area for heat transfer. It was discovered that at a pipe length of 47 m, the outlet temperature was 4.6°C lower than the entrance temperature. In addition, it can be said that the variation of the number of turns does not affect the temperature drop. Another influencing parameter is the pressure drop. The pressure drop generated for each addition of turn is ± 3.5 Pa. The effect of soil types where the EAHE istalled shows that a drop in outlet air temperature is directly proportional to the diffusivity values of the soil. It was found that the outlet air temperature of EAHE downs to 26.141°C for the soil with a thermal diffusivity of 3.37×10^{-7} m^2/s. Finally, the average house temperature using an earth-air heat exchanger has reduced the temperature by 2 °C with an average temperature of 30.4°C. Further studies on the experimental study of EAHE should be conducted in order to validate the model and to investigate a number of crucial parameters, such as air humidity, which are unable to conduct by simulation.

Abbreviation

Symbol	Description
Q_{total}	Heat received or released (J)
$\dot{m}_{air}$	Mass flow rate (kg/s)
$C_{p,air}$	Specific heat value of air (J/kg-K)
$T_{air,out}$	Pipe outlet air temperature (K)
$T_{air,in}$	Pipe inlet air temperature (K)
H	Convection coefficient (W/Mk)
A	Heat transfer area (m^2)
T_{wall}	Soil temperature (K)
$T_{air,out}$	Outlet air temperature (K)
$T_{air,in}$	Inlet air temperature (K)
$T(0,t)$	Surface soil temperature (°C)
T_{mean}	Annual average soil temperature (°C)
A	The amplitude of the temperature wave at the ground surface (z = 0) (°C)
T	Time (days)
$T(0,t)$	Surface soil temperature (°C)
t_0	Time phase constant minimum temperature at soil surface (days)
Z	Soil depth (meters)
d	damping depth ($1/e$ = 0,37)
ω	Frequency of annual temperature waves (2π/time period)/hour
h_{ext}	External heat transfer coefficient
T_{ext}	External heat sink temperature
q_{rad}	Radiative heat flux
ρ_g	The reflectivity of the ground.
ϵ	The angle of inclination of the surface (in degrees) from the horizontal.

Acknowledgement

The authors wish to acknowledge with many thanks to Universitas Syiah Kuala, Minister of National Education for financing the research through the H-Index Grant Program: Publication scheme 2022 No.:144/UN11/SPK/PNBP/2022.

References

[1] V. Murray and K. L. Ebi, "IPCC special report on managing the risks of extreme events and disasters to advance climate change adaptation (SREX)," vol. 66, ed: BMJ Publishing Group Ltd, 2012, pp. 759-760.

[2] N. Rosa, N. Soares, J. Costa, P. Santos, and H. Gervásio, "Assessment of an earth-air heat exchanger (EAHE)

system for residential buildings in warm-summer Mediterranean climate," *Sustainable Energy Technologies and Assessments*, vol. 38, p. 100649, 2020.
[3] O. E. Indonesia, "Badan Pengkajian Dan Penerapan Teknologi," ed: Indonesia, 2013.
[4] A. Lapertot, M. Cuny, B. Kadoch, and O. Le Métayer, "Optimization of an earth-air heat exchanger combined with a heat recovery ventilation for residential building needs," *Energy and Buildings*, vol. 235, p. 110702, 2021/03/15/ 2021, doi: https://doi.org/10.1016/j.enbuild.2020.110702.
[5] Y. O. Saragih, "Uji Eksperimental dan Analisa Sebuah Alat Penukar Kalor Udara-Tanah (Earth-Air Heat Exchanger) dengan Siklus Terbuka," 2017.
[6] S. E. Sofyan, E. Hu, A. Kotousov, T. M. Indra Riayatsyah, Khairil, and Hamdani, "A new approach to modelling of seasonal soil temperature fluctuations and their impact on the performance of a shallow borehole heat exchanger," *Case Studies in Thermal Engineering*, vol. 22, p. 100781, 2020/12/01/ 2020, doi: https://doi.org/10.1016/j.csite.2020.100781.
[7] T. Manik, T. B. Sitorusa, and A. Syahputra, "Performansi Alat Penukar Kalor Udara-Tanah Menggunakan Siklus Tertutup di Kota Medan," *Jurnal Sistem Teknik Industri*, vol. 22, no. 1, pp. 63-76, 2020.
[8] A. Mermoud, "Cours de physique du sol," *Note de cours, Ecole Polytechnique Fédérale de Lausanne, France*, 2006.
[9] B. R. Becker, A. Misra, and B. A. Fricke, "Development of correlations for soil thermal conductivity," *International Communications in Heat and Mass Transfer*, vol. 19, no. 1, pp. 59-68, 1992.
[10] T. Kusuda and J. Bean, "Simplified methods for determining seasonal heat loss from uninsulated slab-on-grade floors," *ASHRAE Trans.;(United States)*, vol. 90, no. CONF-840124-, 1984.
[11] V. Stoichkov, N. Bristow, J. Troughton, F. De Rossi, T. M. Watson, and J. Kettle, "Outdoor performance monitoring of perovskite solar cell mini-modules: Diurnal performance, observance of reversible degradation and variation with climatic performance," *Solar Energy*, vol. 170, pp. 549-556, 2018/08/01/ 2018, doi: https://doi.org/10.1016/j.solener.2018.05.086.
[12] D. Belatrache, S. Bentouba, and M. Bourouis, "Numerical analysis of earth air heat exchangers at operating conditions in arid climates," *International journal of hydrogen energy*, vol. 42, no. 13, pp. 8898-8904, 2017.
[13] M. De Paepe and A. Janssens, "Thermo-hydraulic design of earth-air heat exchangers," *Energy and buildings*, vol. 35, no. 4, pp. 389-397, 2003.
[14] I. M. J. Waisnawa and I. M. B. Pramana, "Pengaruh Pola Ruang Terbuka Hijau Terhadap Sirkulasi Udara Pada Rumah Tinggal," *Segara Widya: Jurnal Penelitian Seni*, vol. 7, no. 1, pp. 17-30, 2019.
[15] W. P. Jones, *Air conditioning engineering*. Routledge, 2007.
[16] K. K. Agrawal, M. Bhardwaj, R. Misra, G. Das Agrawal, and V. Bansal, "Optimization of operating parameters of earth air tunnel heat exchanger for space cooling: Taguchi method approach," *Geothermal Energy*, vol. 6, no. 1, p. 10, 2018/06/21 2018, doi: 10.1186/s40517-018-0097-0.